PAPER • OPEN ACCESS

Rotation of exciton-polariton condensates with TE-TM splitting in a microcavity ring

To cite this article: Chuanyi Zhang and Guojun Jin 2017 *New J. Phys.* **19** 093002

New Journal of Physics
The open access journal at the forefront of physics

Deutsche Physikalische Gesellschaft DPG
IOP Institute of Physics

Published in partnership with: Deutsche Physikalische Gesellschaft and the Institute of Physics

OPEN ACCESS

RECEIVED
10 March 2017

REVISED
27 June 2017

ACCEPTED FOR PUBLICATION
28 July 2017

PUBLISHED
5 September 2017

PAPER

Rotation of exciton-polariton condensates with TE-TM splitting in a microcavity ring

Chuanyi Zhang[1] **and Guojun Jin**[2]

[1] Henan Key Laboratory of Photovoltaic Materials and School of Physics and Electronics, Henan University, Kaifeng, 475004, People's Republic of China
[2] Collaborative Innovation Center of Advanced Microstructures, National Laboratory of Solid State Microstructures, and Department of Physics, Nanjing University, Nanjing, 210093, People's Republic of China

E-mail: chyzhang@henu.edu.cn

Keywords: exciton polariton, TE-TM splitting, rotating condensates

Abstract

We investigate exciton-polariton condensates with a rotating potential induced by an electric field in a semiconductor microcavity ring. In the absence of transverse-electric-transverse-magnetic (TE-TM) splitting, we find that there is a critical laser pump rate, above which the quantized phase slips appear with hysteresis, and there exist quantized average angular momenta at fixed angular velocities, regardless of the pump rate. When considering the TE-TM splitting, we find that there are a series of hysteresis loops with the same intervals which are modulated by the magnitude of the splitting for a linear polarization laser. Further, multistability occurs at large pump rate, and there arises a phase slip for only one spin with large absolute value of the polarization degree, owing to the competition of the TE-TM splitting and energy induced by rotation. These results can be verified experimentally with current technology, and are useful for future electro-optic devices.

1. Introduction

Exciton polaritons (EPs) are quasiparticles resulting from the strong coupling between excitons and photons in a semiconductor microcavity which is a sandwich structure with quantum wells embedded between two Bragg mirrors. Thus EPs can be understood as the quantum superposition of excitons and photons and possess a number of properties that are different from either of the two constituents. The photonic component makes EPs extremely light (about $10^{-5}m_0$ with m_0 being the mass of a free electron), and this unique feature leads to a very high critical temperature for coherent effects, for instance, the coherence of condensates remains at room temperature when the quantum wells are grown with wide-band gap inorganic semiconductors, such as GaN [1] and ZnO [2], or organic materials [3]. While the excitonic component is responsible for the strong nonlinear interactions between EPs, and interestingly, the interactions are spin dependent. Specifically, EPs repel each other in the triplet configuration while attract in the singlet configuration, and the intensity in the latter is much smaller than that in the former. Hence, many intriguing phenomena are attributed to the characteristics [4–6].

To further study the properties of EPs, one may introduce transverse-electric-transverse-magnetic (TE-TM) splitting which can be interpreted as a kind of spin–orbit coupling [7] in a microcavity. This splitting brings about lots of physical effects, such as the optical spin Hall effect [8, 9], optical Berry-phase interferometer [7], topological spin Meissner effect [10], and half-skyrmion spin textures [11]. Besides, the topological properties of EPs have been discussed with the TE-TM splitting in different structures [12–15].

Recently, hysteresis has been observed experimentally in a rotating atomic Bose–Einstein condensate [16], which is considered to be very important in theoretical and practical researches [17]. Due to nonlinear interactions, hysteresis also appears in the EP condensates [18], and the hysteresis loops can be modulated by an external Zeeman field [19]. In this paper, we propose a method to generate the rotating EP condensates and study nonlinear effects with the TE-TM splitting, which has not been considered so far. The results are beneficial

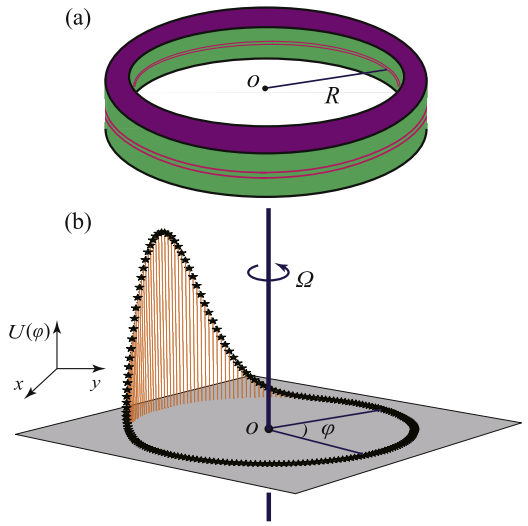

Figure 1. (a) Schematic illustration of a semiconductor microcavity ring with the radius R, and (b) the potential rotates about the axis through the center and perpendicular to the plane of the ring.

for comprehending the coherence in the rotating driven-dissipative systems and developing the optoelectronic devices.

2. Model and formulation

2.1. A possible experimental method

To investigate rotating EP condensates, we should provide a method to realize such systems. An experimentally feasible method may be to rotate a potential of EPs, so we need to consider how to create this kind of potential. According to previous literature, there are several methods to trap EPs, such as a metal mask deposited on the surface of a semiconductor microcavity [20, 21], application of local strain [22, 23], and fabrication of micropillar cavities [24]. In addition, there is a time-dependent trapping potential generated by the surface acoustic waves [25–27]. By analyzing the above methods, we find that they are not suitable for generating a rotating potential. However, there exists a common ground that these methods make the energy of excitons or photons different in real space, which is important for us to find a practical method.

Using an electric field is a possible way to create a rotating potential for EP condensates. As we know, an electric field has an important effect on the energy of excitons, specifically, it can reduce the overlap of electron and hole wavefunctions in quantum wells, which leads to the reduced vacuum Rabi splitting between excitons and photons. Recent experiments have shown the influence of an electric field on the energy of EPs [28, 29]. Additionally, it is found that an external electric field can be used to directly control the spin of an EP condensate and emission polarization [30]. A time-dependent electric field can also change the energy of excitons in a quantum well [31], and the variation of energy is able to be applied to realize the rotating potential.

A semiconductor microcavity is fabricated in the shape of a circular ring with the radius being about 20 μm, as presented in figure 1(a). A recent experiment has been carried out in this structure [32], and the researchers have studied the polarization rotation around the ring and observed the half-quantum circulation in the condensate. However, we investigate EP condensates with a rotating potential which is created by a rotating electric field with the angular velocity Ω in the microcavity ring (figure 1(b)). When the intensity of the excitation laser is large, the EP condensates appear for the opposite spins, and the coherence time is of the order of hundreds of picoseconds. In addition, the superfluid states will be affected by the rotating potential. To study the properties of the condensates, one should collect the EP luminescence in the direction perpendicular to the plane of the ring and analyze it via the real space and dispersion imaging techniques. The condensate phases can be extracted by the Michelson interferometer.

2.2. Formulation

Taking into account the dissipation and replenishment of EPs, nonlinear interactions, and TE-TM splitting, we obtain the Gross–Pitaevskii equations in the rotating frame of reference ($\hbar = 1$),

$$\mathrm{i}\frac{\partial}{\partial t}\Psi_\sigma = -\Theta\frac{\partial^2}{\partial\varphi^2}\Psi_\sigma + \mathrm{i}\Omega\frac{\partial}{\partial\varphi}\Psi_\sigma - \frac{\mathrm{i}}{2}[\gamma_c - \kappa(n_\sigma)]\Psi_\sigma + [U(\varphi) + \eta_1|\Psi_\sigma|^2 + \eta_2|\Psi_{\bar\sigma}|^2 + \eta_3 n_\sigma + \eta_4 n_{\bar\sigma}] \times \Psi_\sigma + \chi \mathrm{e}^{-2\tau_\sigma \mathrm{i}\varphi}\left(\frac{\partial^2}{\partial\varphi^2} - 2\tau_\sigma \mathrm{i}\frac{\partial}{\partial\varphi}\right)\Psi_{\bar\sigma}, \quad (1)$$

$$\frac{\partial}{\partial t}n_\sigma = P_\sigma(\varphi) - \gamma_r n_\sigma - \kappa(n_\sigma)|\Psi_\sigma|^2, \quad (2)$$

where Ψ_σ is the order parameter of EP condensates with σ being the spin index, and $\bar\sigma$ represents the opposite spin to σ. Besides, $\tau_\uparrow = 1$ and $\tau_\downarrow = -1$. The constant Θ is equal to $1/(2mR^2)$ (about 1.9 μ eV), where m labels the effective mass of EPs, and χ denotes the magnitude of the TE-TM splitting. Owing to the loss of EPs at a rate γ_c, EPs should be replenished by a reservoir with the density n_σ in the steady state, and $P_\sigma(\varphi)$ and γ_r are the laser pump rate and dissipation rate of EPs in reservoirs. The term $\kappa(n_\sigma)$ is the stimulated scattering rate from the reservoirs to condensates, and is approximatively proportional to the density n_σ [33, 34]. The parameters η_1 (η_2) and η_3 (η_4) are the interaction constants of EPs in condensates and between condensates and reservoirs in the triplet (singlet) configuration, respectively.

The potential $U(\varphi)$ is time independent in the rotating coordinate system, and written as

$$U(\varphi) = U_0 \exp[-4(\varphi - \pi)^2], \quad (3)$$

where U_0 is a constant and equal to 200Θ throughout this work. This potential makes EP condensates rotate, which will affect the properties of condensates.

3. Results and discussion

The steady states are discussed in the system, and we introduce the chemical potential μ in the usual way and have the expression $\mathrm{i}\partial_t\Psi_\sigma = \mu\Psi_\sigma$. Here the parameter μ is determined from the balance of gain and loss. Two cases are distinguished to study the rotating EP condensates, that is, neglecting and taking into account the TE-TM splitting, and the effect of this splitting will emerge by comparison. Additionally, we should point out that the potential $U(\varphi)$ is created by an electric field, and the non-condensed EPs are also affected in reservoirs, so we treat the pump rate $P_\sigma(\varphi)$ as its average in the microcavity ring.

3.1. No TE-TM splitting

We first consider a simple case that there is no TE-TM splitting (i.e., $\chi = 0$), and the states are degenerate for the opposite spins. Thus one gets $\Psi_\uparrow = \Psi_\downarrow$ in this case, and Ψ_σ is written as $\Psi_\sigma = \sqrt{\rho_\sigma}\exp(\mathrm{i}\Phi_\sigma)$. The superfluid velocity is defined from the phases of condensates, i.e., $\zeta_\sigma = (mR)^{-1}\partial\Phi_\sigma/\partial\varphi$, and it is easily influenced by the angular velocity.

By numerical calculations, we find that the angular velocity Ω has little effect on the condensate densities which are greatly influenced by the potential. However, the condensate phases are very sensitive to the angular velocity, as shown in figure 2(a). If the angular velocity is small, we obtain an expression, $\Phi(0) = \Phi(2\pi)$. The value of $\Phi(2\pi) - \Phi(0)$ is 2π for larger Ω. To discuss this phenomenon, we introduce the topological winding number which reads $W_\sigma = \int_0^{2\pi}\partial_\varphi\Phi_\sigma \mathrm{d}\varphi/(2\pi)$. It is easy to obtain the expressions, i.e., $W_\sigma = 0$ for $\Omega = 0.5\Theta$, and $W_\sigma = 1$ for $\Omega = 1.5\Theta$ or 2Θ.

The superfluid velocity can help us to get more information about the condensate phases in figure 2(b), and we discuss the physical quantities in the rotating frame of reference. For a fixed angular velocity, the variation of ζ_σ is obvious in the potential barrier region, as illustrated in figure 1(b). In the remaining region, ζ_σ is almost unchanged and approximatively equal to W_σ, in other words, the phases increase approximately linearly with the angle φ. As the angular velocity rises, ζ_σ becomes large except the potential barrier region.

When the EP condensates rotate, it is necessary to discuss the average angular momentum which has the expression,

$$\Gamma_\sigma = \frac{\int_0^{2\pi}\rho_\sigma\partial_\varphi\Phi_\sigma \mathrm{d}\varphi}{\int_0^{2\pi}\rho_\sigma \mathrm{d}\varphi}. \quad (4)$$

From equation (4), we can see that the average angular momenta are mainly determined by the condensate phases for the opposite spins, while the phases can be regulated by the angular velocity. Hence the angular momenta will be greatly affected by the angular velocity. In this system, Ψ_σ has the expression, $\Psi_\sigma = \psi_\sigma\exp(\mathrm{i}j\varphi)$ with j being an integer. If the pump rate is small, the average angular momenta increase with the angular velocity, and the winding numbers directly jump from j to $j+1$ at certain angular velocities Ω_0, that is, the quantized

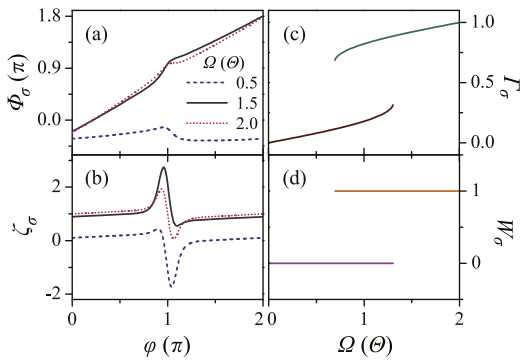

Figure 2. The condensate phases Φ_σ and superfluid velocities ζ_σ as a function of the angle φ with different angular velocities in the left panels, and the average angular momenta Γ_σ and winding numbers W_σ varying with the angular velocity Ω in the right panels. $P_\uparrow = P_\downarrow = 5000\Theta$ in all the figures.

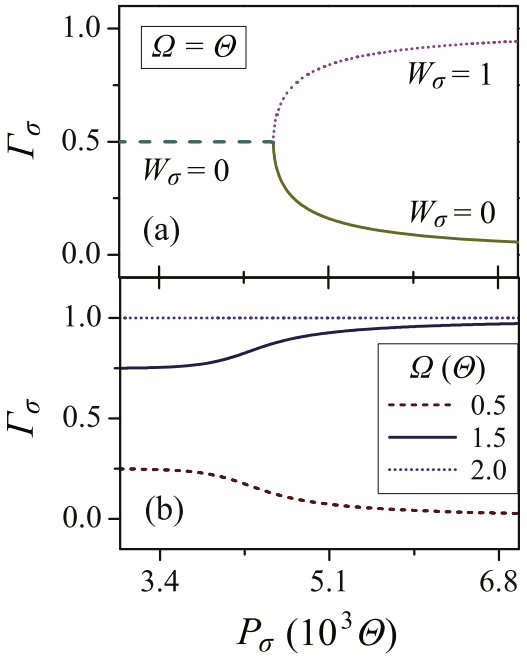

Figure 3. The average angular momenta Γ_σ varying with the pump rate P_σ with different angular velocities.

phase slips take place. When we substitute the factor of condensate phases into equation (1), a valuable expression is obtained,

$$\Omega_0 = (2j + 1)\Theta, \tag{5}$$

and thus the winding numbers jump with a period 2Θ. When the pump rate is large, hysteresis arises by varying the angular velocity, which is reflected on the average angular momenta and winding numbers, and Ω_0 lies at the center of the hysteresis loops. As the angular velocity continues to increase, there emerge periodic hysteresis loops with the interval 2Θ, and phase slips appear with hysteretic behavior.

When the pump rate varies, the condensate densities and phases are influenced, which leads to the variation of the average angular momenta. From the above discussion, we find that the winding numbers jump directly from 0 to 1 at $\Omega = \Theta$ with small pump rate, and hysteresis arises for larger P_σ. Hence it is interesting to study the average angular momenta at $\Omega = \Theta$ by varying the pump rate, as shown in figure 3(a). Γ_σ and W_σ are both unchanged for smaller P_σ, which can be explained by the fact that the densities of condensates are symmetrical in the ring, namely, $\rho_\sigma(\pi - \varphi) = \rho_\sigma(\pi + \varphi)$, and the average values of superfluid velocities are equal to 0.5. According to equation (4), the average angular momenta are about 0.5 and almost unchanged. Importantly, there is a critical pump rate P_c for hysteresis, that is, only one steady state exists if $P_\sigma < P_c$, and two states appear if $P_\sigma > P_c$. As P_σ continues to increase, Γ_σ first goes up fast and then slowly in the upper state with $W_\sigma = 1$, while it reduces gradually in the lower state with $W_\sigma = 0$.

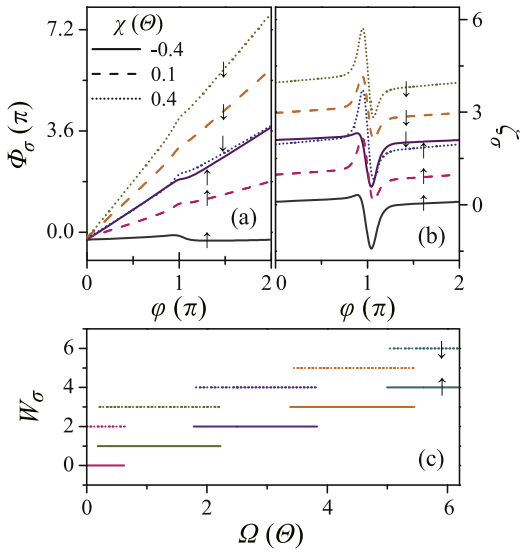

Figure 4. The condensate phases Φ_σ and superfluid velocities ζ_σ versus the angle φ with different magnitudes of the TE-TM splitting in the upper panels, and the winding numbers W_σ as a function of the angular velocity Ω in the lower panel. The different spins are marked on the lines in (a) and (b), and $\Omega = 1.5\Theta$. The solid and dotted lines represent the spin up and spin down, respectively, in (c), and $\chi = 0.2\Theta$. $P_\uparrow = P_\downarrow = 5000\Theta$ in all the figures.

If the angular velocity lies out of the hysteresis loop in figure 2(c), the average angular momenta can be changed by the pump rate for different angular velocities in figure 3(b), to be specific, when P_σ rises, Γ_σ decreases slowly if $0 < \Omega < \Theta$, and increases in the interval $(\Theta,\ 2\Theta)$. But Γ_σ is almost unchanged for smaller pump rate, which mainly comes from the unaltered superfluid velocity. Note that there is a specific angular velocity, i.e., $\Omega = 2\Theta$, at which the average angular momenta are constants and not influenced by the pump rate. Besides, the winding numbers are still a single value and unchanged with the variation of P_σ.

A different scenario has been put forward to stir the EP condensate by using a laser field carrying orbital angular momentum, and persistent currents and quantized vortices have been observed in the experiment [35]. In the work, the winding number of the vortices is mainly influenced by the excitation laser. In our system, persistent currents appear if there is a rotating potential, and the winding number is determined by the angular velocity and interactions between EPs without the TE-TM splitting.

3.2. With TE-TM splitting

When we consider the TE-TM splitting in the microcavity ring, the degenerate states are broken, and the condensate phases are different for the opposite spins. For a given microcavity, the magnitude of the TE-TM splitting χ can be modulated by the detuning of the microcavity mode with respect to the center of the stop band of the distributed Bragg mirrors [36, 37]. A giant splitting has been achieved by using an organic microcavity [38, 39] or a tunable open microcavity [40], and this result is conducive to investigating the novel quantum phenomena.

The condensate densities are almost immune to the TE-TM splitting, while the phases are greatly influenced by it with the linearly polarized exciting laser, i.e., $P_\uparrow = P_\downarrow$, which can be seen from equations (1) and (2). In figure 4(a), χ has a great effect on the phases for the opposite spins, e.g., $\Phi_\uparrow(2\pi) - \Phi_\uparrow(0)$ is equal to 0, 2π, and 4π at $\chi = -0.4\Theta$, 0.1Θ, and 0.4Θ, respectively. Accordingly, $\Phi_\downarrow(2\pi) - \Phi_\downarrow(0)$ is 4π, 6π, and 8π. The difference of phases can be discussed by the winding numbers, and $W_\uparrow$ ($W_\downarrow$) is 0 (2), 1 (3), and 2 (4) at the corresponding value of χ. It is evident that we can obtain an expression, $W_\downarrow - W_\uparrow = 2$, since this result directly comes from the TE-TM splitting. This splitting greatly affects the properties of EP condensates and makes the warping of half-quantum vortices appear [37]. The superfluid velocities, reflecting the variation of phases, can be divided into two parts here. One part represents the winding numbers, and the other denotes the small variation of phases in ψ. From figure 4(b), we can see that the former is greatly influenced by χ, while the latter is not sensitive to it, and the variation of the latter is similar to that in figure 2(b). Hence, the winding numbers which are affected by the TE-TM splitting play an important role in the superfluid velocities.

For a fixed χ, the average angular momenta increase as the angular velocity becomes large, and there are still hysteresis loops for each spin. In figure 4(c), the winding numbers are shown with several loops. Comparing with the results in figure 2(d), we find that the winding number increases by two for spin down, which stems from the factor $\exp(\pm 2i\varphi)$ in equation (1). There are more loops as the angular velocity rises, and the intervals of adjacent loops are the same. By analysis, the order parameters can be expressed as, $\Psi_\uparrow = \psi_\uparrow \exp(iW_\uparrow\varphi)$ and

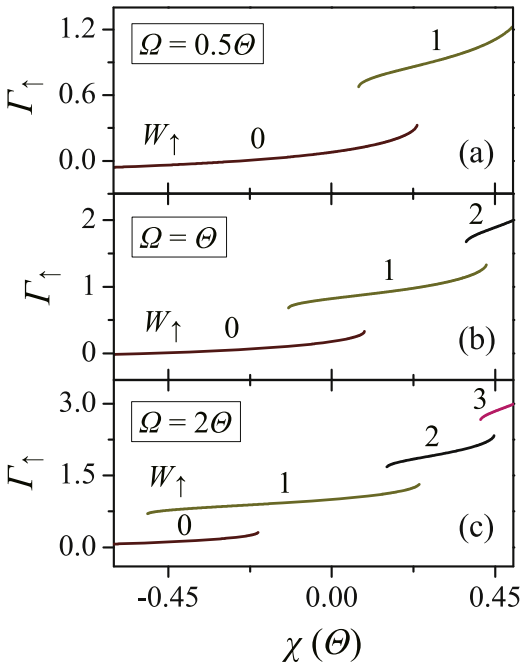

Figure 5. The average angular momentum $\Gamma_\uparrow$ varying as a function of the magnitude of the TE-TM splitting χ with different angular velocities. The numbers, labeled on the lines, denote the winding number $W_\uparrow$ in the corresponding regions of χ. $P_\uparrow = P_\downarrow = 5000\Theta$.

$\Psi_\downarrow = \psi_\downarrow \exp(\mathrm{i}W_\downarrow\varphi)$, with the TE-TM splitting. When these expressions are substituted into equation (4), we obtain the interval λ of adjacent loops,

$$\lambda = 2(1 - \chi)\Theta. \tag{6}$$

From equation (6), we can see that the interval is related with the TE-TM splitting, which agrees with the numerical results. Besides, the difference of average angular momenta reads,

$$\Gamma_\downarrow - \Gamma_\uparrow = W_\downarrow - W_\uparrow = 2, \tag{7}$$

and it is independent of the magnitude of the TE-TM splitting, so we can only take into account one spin with the linearly polarized laser.

To reflect the effect of the TE-TM splitting on hysteresis, we change the magnitude of the splitting and display the results for spin up in figure 5. The average angular momentum $\Gamma_\uparrow$ rises with the increasing TE-TM splitting, and hysteresis appears in some regions. When the angular velocity is small, there is only one hysteresis loop, and the width of the loop is about 0.16Θ in figure 5(a). As Ω becomes large, there appear more hysteresis loops with the variation of χ, e.g., two loops at $\Omega = \Theta$ and three loops at $\Omega = 2\Theta$. In figure 5(c), the winding number $W_\uparrow$ jumps from 0 to 1, 1 to 2, and 2 to 3 at the first, second, and third loop, respectively. The width of the loops is about 0.3Θ, 0.09Θ, and 0.04Θ, respectively, so it becomes small as χ goes up, and simultaneously, the interval of adjacent loops reduces.

When the pump rate is small, there are no hysteresis loops, and the average angular momenta increase continuously. Besides, the winding numbers jump directly at fixed points, for instance, if $\Omega = 2\Theta$, these points are about $\chi = -0.35\Theta$, 0.2Θ, and 0.43Θ, respectively. When the pump rate is large, all the hysteresis loops emerge, and the centers of the loops are still at these points, which is not affected by the pump rate. Thus the position of the center of loops is determined by the angular velocity and magnitude of the TE-TM splitting.

In the above discussion, we only consider a linearly polarized laser, and the TE-TM splitting has an important effect on the properties of condensates. If an elliptically polarized laser is applied, the phenomena may be different. We define the circular polarization degree of an excitation laser, $\nu = (P_\uparrow - P_\downarrow)/(P_\uparrow + P_\downarrow)$, and the polarization will affect greatly the condensate densities and phases [41]. If $\nu > 0$, $\rho_\uparrow$ is larger than $\rho_\downarrow$, and their difference becomes large with the increasing ν, as can be seen from equations (1) and (2).

For the small pump rate, the winding numbers are unchanged with small ν, while the average angular momenta have different variations for the opposite spins, i.e., $\Gamma_\uparrow$ decreases gradually, but $\Gamma_\downarrow$ rises as ν goes up. When the pump rate is large, there exist different phenomena, as shown in figure 6. When we fix the angular velocity Ω and change the magnitude of the TE-TM splitting, there are two states at $\chi = 0.3\Theta$, namely, $(W_\uparrow, W_\downarrow) = (1, 3)$ (denoted by case 1) and $(W_\uparrow, W_\downarrow) = (2, 4)$ (denoted by case 2). When the value of $|\nu|$ is small, we find that more states emerge for case 1, to be specific, there are three states, $(W_\uparrow, W_\downarrow) = (1, 3)$,

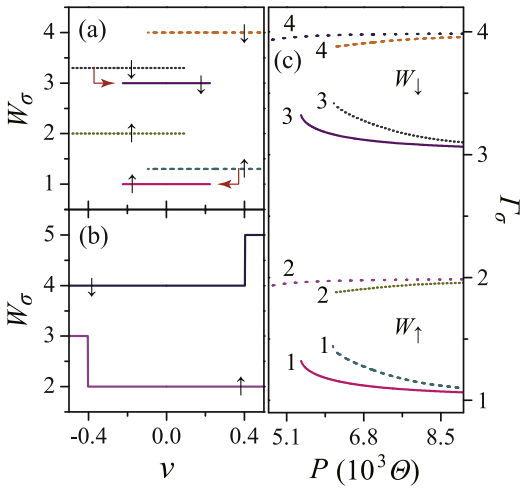

Figure 6. The winding numbers W_σ varying with the polarization degree ν in left panels, and the average angular momenta Γ_σ versus the pump rate in the right panel. One state is denoted by the same two lines (marked by spin up and down), and the winding numbers are given in every state in (c). The pump rate is $P(1+\nu)$ and $P(1-\nu)$ for spin up and spin down, respectively, and $P = 7000\Phi$ in (a) and (b), and $\nu = 0$ in (c). $\Omega = 2\Theta$ and $\chi = 0.3\Theta$ in all the panels.

$(W_\uparrow, W_\downarrow) = (1, 4)$, and $(W_\uparrow, W_\downarrow) = (2, 3)$, if $|\nu| < 0.1$, and this is multistability. This effect emerges due to the nonlinear interactions, and it also takes place in the absence of the TE-TM splitting [42]. If ν locates in the interval $(-0.22, -0.1)$ or $(0.1, 0.22)$, two states exist, and this is bistability in figure 6(a). As $|\nu|$ becomes larger, only one state remains, that is, $(W_\uparrow, W_\downarrow) = (1, 4)$ or $(W_\uparrow, W_\downarrow) = (2, 3)$. For case 2, there is only one state as the polarization degree varies, and $(W_\uparrow, W_\downarrow) = (2, 4)$ directly jumps to $(3, 4)$ and $(2, 5)$ at $\nu = -0.4$ and $\nu = 0.4$, respectively, in figure 6(b). An electrical spin switch has been realized recently [30], and the spin bifurcation can be promoted by an electric field. There are differences between the spin bifurcation and the multistability discussed here in the presence of the TE-TM splitting, for example, the spin bifurcation forms due to the anisotropy of the nonlinear interactions, and a polarization state can be selected deterministically by the pump intensities in multistability.

From figure 6(a), we can see that the winding numbers jump with hysteresis as the polarization degree varies, in other words, the quantum phase slips arise with hysteretic effect. For case 2, there also exist phase slips, but without hysteretic behavior. It should be noted that new states appear with large $|\nu|$ for both cases, and the winding numbers may be different from the their initial values, although there are hysteresis loops. The phase slip exists for one spin, and the winding number is unchanged for the other spin. This phenomenon can be explained as follows, when $|\nu|$ is little, the difference of the densities is small for the opposite spins, so the winding numbers are mainly determined by the angular velocity Ω, and the TE-TM splitting makes $W_\downarrow - W_\uparrow$ equal 2, as shown in equation (1). If $|\nu|$ becomes large, the effect of the splitting is different for the opposite spins, for example, the density $\rho_\uparrow$ is larger than $\rho_\downarrow$ at positive ν, so the effect of the splitting becomes weak for spin up, and $W_\uparrow$ is dependent on Ω. While for spin down, the splitting is strong and makes $W_\downarrow$ increase. Therefore, there exists a competition between the TE-TM splitting and energy induced by rotation for the winding numbers.

When the polarization degree is fixed, the variation of the average angular momenta is small by varying the pump rate, as shown in figure 6(c). As the pump rate decreases, there are four states, $(W_\uparrow, W_\downarrow) = (1, 3)$, $(2, 4)$, $(2, 3)$, and $(1, 4)$, which agree with the results in the left panels of figure 6, and then two states remain, i.e., $(1, 3)$ and $(2, 4)$. At last, there is only one state, namely, $(W_\uparrow, W_\downarrow) = (2, 4)$, for the smaller pump rate. This phenomena result from the width of hysteresis loops in figure 6(a). Besides, $\Gamma_\uparrow$ and $\Gamma_\downarrow$ have the similar variations in the states $(W_\uparrow, W_\downarrow) = (1, 3)$ and $(2, 4)$, and have different variations for the other states.

4. Conclusion

We have studied the EP condensates rotating around the axis through the center and perpendicular to the plane of the microcavity ring. In the absence of TE-TM splitting, we find that there exists a critical pump rate, above which the quantized phase slips occur with hysteretic effect, and there are quantized average angular momenta at the fixed angular velocities, which is independent of the pump rate. When the TE-TM splitting is fully taken into account, the winding numbers, as well as the average angular momenta, are affected. We find that there are a series of hysteresis loops with the same intervals which are determined by the magnitude of the TE-TM splitting for a linear polarization laser. In addition, the hysteretic behavior also appears by varying the magnitude of the

splitting. When an elliptically polarized laser is applied, we find that multistability occurs for large pump rate with small absolute value of the polarization degree, while only one state exists at small pump rate. For large absolute value of the polarization degree, there emerges a phase slip for one spin, and the winding number of the other spin is unchanged, which can be explained by the competition of the TE-TM splitting and the energy induced by rotation. These results can be verified experimentally with current technology, and are useful in electro-optic devices.

Acknowledgments

This work was supported by the National Natural Science Foundation of China (Grant No. 61504039), Key Research Plan in University of Henan Province (Grant No. 15A140018), and State Key Program for Basic Research of China (Grant No. 2015CB921202).

References

[1] Levrat J, Butté R, Christian T, Glauser M, Feltin E, Carlin J-F, Grandjean N, Read D, Kavokin A V and Rubo Y G 2010 *Phys. Rev. Lett.* **104** 166402
[2] Franke H, Sturm C, Schmidt-Grund R, Wagner G and Grundmann M 2012 *New J. Phys.* **14** 013037
[3] Plumhof J D, Stöferle T, Mai L, Scherf U and Mahrt R F 2014 *Nat. Mater.* **13** 247
[4] Shelykh I A, Kavokin A V, Rubo Y G, Liew T C H and Malpuech G 2010 *Semicond. Sci. Technol.* **25** 013001
[5] Carusotto I and Ciuti C 2013 *Rev. Mod. Phys.* **85** 299
[6] Zhang C, Zhang Y and Jin G 2011 *J. Appl. Phys.* **109** 053509
[7] Shelykh I A, Pavlovic G, Solnyshkov D D and Malpuech G 2009 *Phys. Rev. Lett.* **102** 046407
[8] Kavokin A, Malpuech G and Glazov M 2005 *Phys. Rev. Lett.* **95** 136601
[9] Leyder C, Romanelli M, Karr J P, Giacobino E, Liew T C H, Glazov M M, Kavokin A V, Malpuech G and Bramati A 2007 *Nat. Phys.* **3** 628
[10] Gulevich D R, Skryabin D V, Alodjants A P and Shelykh I A 2016 *Phys. Rev.* B **94** 115407
[11] Cilibrizzi P *et al* 2016 *Phys. Rev.* B **94** 045315
[12] Masumoto N, Kim N Y, Byrnes T, Kusudo K, Löffler A, Höfling S, Forchel A and Yamamoto Y 2012 *New J. Phys.* **14** 065002
[13] Kim N Y, Kusudo K, Löffler A, Höfling S, Forchel A and Yamamoto Y 2013 *New J. Phys.* **15** 035032
[14] Karzig T, Bardyn C, Lindner N H and Refael G 2015 *Phys. Rev.* X **5** 031001
[15] Solnyshkov D D, Nalitov A V and Malpuech G 2016 *Phys. Rev. Lett.* **116** 046402
[16] Eckel S, Lee J G, Jendrzejewski F, Murray N, Clark C W, Lobb C J, Phillips W D, Edwards M and Campbell G K 2014 *Nature* **506** 200
[17] Davis M J and Helmerson K 2014 *Nature* **506** 166
[18] Baas A, Karr J P, Eleuch H and Giacobino E 2004 *Phys. Rev.* A **69** 023809
[19] Zhang C and Zhang W 2015 *Phys. Lett.* A **379** 1766
[20] Lai C W *et al* 2007 *Nature* **450** 529
[21] Kim N Y, Kusudo K, Wu C, Masumoto N, Löffler A, Höfling S, Kumada N, Worschech L, Forchel A and Yamamoto Y 2011 *Nat. Phys.* **7** 681
[22] Balili R, Hartwell V, Snoke D, Pfeiffer L and West K 2007 *Science* **316** 1007
[23] Balili R B, Snoke D W, Pfeiffer L and West K 2006 *Appl. Phys. Lett.* **88** 031110
[24] Bajoni D, Senellart P, Wertz E, Sagnes I, Miard A, Lemaître A and Bloch J 2008 *Phys. Rev. Lett.* **100** 047401
[25] de Lima M M, van der Poel J M, Santos P V and Hvam J M 2006 *Phys. Rev. Lett.* **97** 045501
[26] Cerda-Méndez E A, Krizhanovskii D N, Wouters M, Bradley R, Biermann K, Guda K, Hey R, Santos P V, Sarkar D and Skolnick M S 2010 *Phys. Rev. Lett.* **105** 116402
[27] Cerda-Méndez E A, Sarkar D, Krizhanovskii D N, Gavrilov S S, Biermann K, Skolnick M S and Santos P V 2013 *Phys. Rev. Lett.* **111** 146401
[28] Tsotsis P *et al* 2014 *Phys. Rev. Appl.* **2** 014002
[29] Brodbeck S, Suchomel H, Amthor M, Wolf A, Kamp M, Schneider C and Höfling S 2015 *Appl. Phys. Lett.* **107** 041108
[30] Dreismann A, Ohadi H, Redondo Y del V-I, Balili R, Rubo Y G, Tsintzos S I, Deligeorgis G, Hatzopoulos Z, Savvidis P G and Baumberg J J 2016 *Nat. Mater.* **15** 1074
[31] Maslov A V and Citrin D S 2000 *Phys. Rev.* B **62** 16686
[32] Liu G, Snoke D W, Daley A, Pfeiffer L N and West K 2015 *Proc. Natl Acad. Soc.* **112** 2676
[33] Wouters M and Carusotto I 2007 *Phys. Rev. Lett.* **99** 140402
[34] Lagoudakis K G, Wouters M, Richard M, Baas A, Carusotto I, André R, Dang L S and Deveaud-Plédran B 2008 *Nat. Phys.* **4** 706
[35] Sanvitto D *et al* 2010 *Nat. Phys.* **6** 527
[36] Panzarini G, Andreani L C, Armitage A, Baxter D, Skolnick M S, Astratov V N, Roberts J S, Kavokin A V, Vladimirova M R and Kaliteevski M A 1999 *Phys. Rev.* B **59** 5082
[37] Toledo-Solano M, Mora-Ramos M E, Figueroa A and Rubo Y G 2014 *Phys. Rev.* B **89** 035308
[38] Kéna-Cohen S, Davanço M and Forrest S R 2008 *Phys. Rev. Lett.* **101** 116401
[39] Stelitano S, Savasta S, Patané S, De Luca G and Scolaro L M 2009 *J. Appl. Phys.* **106** 033102
[40] Dufferwiel S *et al* 2015 *Phys. Rev. Lett.* **115** 246401
[41] Krizhanovskii D N, Sanvitto D, Shelykh I A, Glazov M M, Malpuech G, Solnyshkov D D, Kavokin A, Ceccarelli S, Skolnick M S and Roberts J S 2006 *Phys. Rev.* B **73** 073303
[42] Gippius N A, Shelykh I A, Solnyshkov D D, Gavrilov S S, Rubo Y G, Kavokin A V, Tikhodeev S G and Malpuech G 2007 *Phys. Rev. Lett.* **98** 236401